

# Communication-Assisted Sensing in 6G Networks

Fuwang Dong, *Member, IEEE*, Fan Liu, *Senior Member, IEEE*, Shihang Lu, Yifeng Xiong, *Member, IEEE*, Qixun Zhang, *Member, IEEE*, Zhiyong Feng, *Senior Member, IEEE*, and Feifei Gao, *Fellow, IEEE*

**Abstract**—Exploring the mutual benefit and reciprocity of sensing and communication (S&C) functions is fundamental to realizing deeper integration for integrated sensing and communication (ISAC) systems. This paper investigates a novel communication-assisted sensing (CAS) system within 6G perceptive networks, where the base station actively senses the targets through device-free wireless sensing and simultaneously transmits the estimated information to end-users. In such a CAS system, we first establish an optimal waveform design framework based on the rate-distortion (RD) and source-channel separation (SCT) theorems. After analyzing the relationships between the sensing distortion, coding rate, and communication channel capacity, we propose two distinct waveform design strategies in the scenario of target impulse response estimation. In the separated S&C waveforms scheme, we equivalently transform the original problem into a power allocation problem and develop a low-complexity one-dimensional search algorithm, shedding light on a notable *power allocation tradeoff* between the S&C waveform. In the dual-functional waveform scheme, we conceive a heuristic mutual information optimization algorithm for the general case, alongside a modified gradient projection algorithm tailored for the scenarios with independent sensing sub-channels. Additionally, we identify the presence of both *subspace tradeoff* and *water-filling tradeoff* in this scheme. Finally, we validate the effectiveness of the proposed algorithms through numerical simulations.

**Index Terms**—Communication-assisted sensing, waveform design, ISAC, sensing-as-a-service, rate-distortion theory.

## I. INTRODUCTION

THE next-generation wireless networks (5G-A and 6G) are envisioned to simultaneously provide high-precision sensing capabilities and ubiquitous wireless connectivity with the help of integrated sensing and communications (ISAC) technology, leading to a perceptive network [2]. Unlike the traditional separate deployment of sensing and communications (S&C) systems, ISAC system is well-recognized for its potential to achieve *integration gain* and *coordination gain* [3], which has been officially approved as one of the six key usage scenarios of 6G by the international telecommunications union (ITU) [4]. Over the past few decades, significant research

efforts have been dedicated to exploring and harnessing the *integration gain*, aiming to enhance S&C performance and improve resource efficiency by the shared use of both wireless resources and hardware platforms. This line of research includes the development of dual-functional ISAC waveforms, beamforming, and transmission protocols (cf. [5]–[8], and the reference therein). Additionally, fundamental theoretical studies depicting the performance bounds of ISAC systems are also well underway [9]–[11]. However, there exists a notable gap in the literature concerning the exploitation of the *coordination gain* offered by the ISAC system.

### A. Sensing-Assisted Communication Framework

As the name implies, the *coordination gain* is achievable through the collaboration of S&C subsystems. As an example, extensive research efforts have been dedicated to efficiently establishing reliable communication links with the support of radar sensing capabilities. Pioneered by [12], a sensing-assisted communication (SAC) framework was proposed to improve the quality of service (QoS) in high-mobility vehicular networks. Within this framework, the motion parameters of the targets are estimated based on the echoes of the dual-functional transmitting signal. In conjunction with the extended Kalman filtering method, the SAC method significantly reduces the signaling overhead and improves the accuracy of parameter estimation by sophisticatedly tailored beam tracking and prediction approaches, outperforming conventional feedback-based beam tracking approaches. Subsequently, the SAC performance was further enhanced by advanced Bayesian inference approaches, which may achieve near-optimal performance through a message passing algorithm [13]. However, it is worth pointing out that these works are based on the assumptions of point-like targets and ideal linear motion models. To address these limitations, the dynamic predictive beamforming for extended targets [14] and the consideration of arbitrarily shaped roads [15] have been explored to enhance reliability in complex environments. Recently, the authors of [16] employ an intelligent omni-surface on the surface of vehicles to further enhance the S&C performance.

While the previous studies have primarily focused on improving communication performance with the aid of sensing, it is crucial to acknowledge that the sensing functionality itself could be a native service provided to a vast number of users in 6G networks. Indeed, sensing-as-a-service is essential to fulfill the requirements of various emerging environment-aware applications such as Internet of Things (IoT), extended reality (XR) services, and autonomous driving [2], [17], [18]. Consequently, a natural question arises: *How can sensing performance be enhanced by incorporating communication functionality in 6G perceptive networks?*

(Corresponding author: Fan Liu.)

Part of this paper was presented at IEEE/CIC International Conference on Communications in China (ICCC) 2023 [1].

Fuwang Dong, Fan Liu, and Shihang Lu are with the School of System Design and Intelligent Manufacturing, Southern University of Science and Technology, Shenzhen 518055, China. (email: dongfw@sustech.edu.cn; liuf6@sustech.edu.cn; lush2021@mail.sustech.edu.cn).

Yifeng Xiong is with the School of Information and Electronic Engineering, Beijing University of Posts and Telecommunications, Beijing 100876, China. (email: yifengxiong@bupt.edu.cn).

Qixun Zhang and Zhiyong Feng are with Key Laboratory of Universal Wireless Communications Ministry of Education, Beijing University of Posts and Telecommunications, Beijing 100876, China. (email: zhangqixun@bupt.edu.cn; email: fengzy@bupt.edu.cn).

Feifei Gao is with Department of Automation, Tsinghua University, Beijing 100876, China. (email: feifeigao@ieee.org).

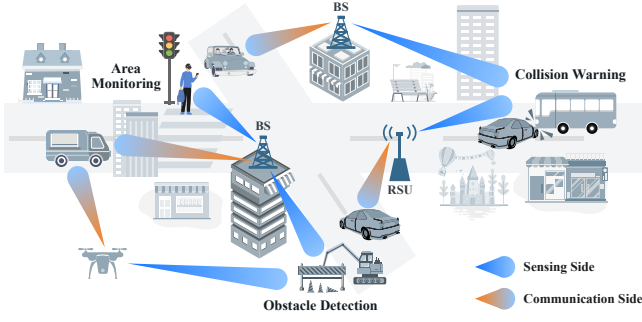


Fig. 1. The BLoS sensing in the proposed CAS system.

### B. Communication-Assisted Sensing Framework

In 6G perceptive networks, users are expected to attain superior beyond-line-of-sight (BLoS) sensing capabilities in conjunction with the proposed communication-assisted sensing (CAS) framework. Here, BLoS sensing refers to the process by which the user acquires the state information of the obstructed or exceptionally distant targets, as shown in Fig. 1. In the CAS process, the base station (BS) or roadside unit (RSU) with favorable visibility illuminates the targets and captures observations (i.e., sensing process). Subsequently, the BS conveys the state information acquired during the sensing stage to the end-users (i.e., communication process). Note that the BLoS sensing capability has explored in the current cellular networks by sharing the sensory data collected by the other sensors. The authors of [19] presented a time duration allocation scheme of S&C to share the raw sensing data acquired by vehicle-mounted sensors among the users. However, it is worth highlighting that the BS in CAS system actively performs *device-free* sensing without the aid of additional sensors, where sensing is the intrinsic capability of the network. Consequently, the S&C performance tradeoff leads to a significantly different working pipeline from the existing schemes and the unique challenges in the CAS system designs.

Specifically, the QoS of BLoS sensing attained by the user depends on both estimation distortion in the sensing process and recovery distortion in the communication process. Therefore, the S&C coupling in the CAS system manifests in the following two aspects. Firstly, S&C performance is determined by system resource management (e.g., power, bandwidth, waveform) since both S&C processes are implemented on the same hardware platform. Secondly, it requires a large number of bits to represent the estimated parameters precisely and a better communication channel capacity to transmit the estimates reliably. Suppose the BS excessively allocates resources to the sensing process for accurate estimation. In this case, the communication channel capacity may not be good enough to transmit such estimates to the user, leading to a QoS degradation. From the information-theoretical perspective, the above-mentioned lossy data transmission can be characterized by the *source-channel separation theorem (SCT)* with distortion and the *rate-distortion (RD)* theory [20].

The similar work related to the above CAS process is referred to remote source coding (also known as the *chief*

*estimation officer (CEO)* problem), where the BS can only access noisy observations rather than the original source information [21], [22]. Two primary approaches in remote source coding are the compress-and-estimate (CE) and estimate-and-compress schemes (EC) schemes. In the CE scheme, the BS directly compresses the received observations and transmits the raw data to the user, with estimation procedures being conducted after compression. By contrast, in the EC scheme, the BS initially estimates the parameters from the observations and then transmits the compressed estimation results to the user according to the available rate. It is widely recognized that the optimal tradeoff between the information rate and the expected distortion is achieved through the EC strategy [23]. In light of this, and by noting the fact that the BS has significantly better signal processing capability than that of the user, we also adopt an EC scheme in this paper, where the BS transmits the estimates to the user.

In remote source coding, explicitly characterizing the distortion and information rate for arbitrary source distribution remains a challenging task. Therefore, extensive attention has been paid to a specific case known as the quadratic Gaussian problem [24]–[27]. Concretely, the target parameters as Gaussian sources undergo linear observations corrupted by additive Gaussian noise, with the minimum mean squared error (MMSE) being employed as the distortion metric. In this scenario, most of the existing works concentrated on performance analysis, as well as the characterization of achievable inner and outer bounds of the rate-distortion region. However, the practical design of transmitting waveform, a crucial aspect in the context of ISAC networks, still remains widely unexplored within the framework of remote source coding. To fill this research gap, our study is dedicated to resolving the following problem: *How can we strategically design a waveform to optimize sensing QoS, while considering the S&C coupling and resource budget constraints in the CAS systems?*

### C. Our Contributions

In this paper, we address the waveform design problem within the context of CAS system in 6G perceptive networks, where the main focus is on achieving optimal sensing QoS at the user end. Our specific attention is directed toward target response matrix (TRM) estimation, with the to-be-estimated parameters being the sensing channel itself. As a result, we may model the EC procedure as a quadratic Gaussian problem. We defer the consideration of waveform design for general radar parameter estimation (e.g., range, Doppler, angle) with arbitrary prior distributions to future research. The main contributions of this paper are summarized as follows.

- First, we establish a CAS framework in 6G perceptive networks based on the theories of the RD and the SCT in lossy data transmission. This framework clearly characterizes the relationship between the distortion, coding rate, and channel capacity. Additionally, we develop the waveform design scheme that minimizes the distortion achieved by the user while adhering to the SCT and power budget constraints.
- Second, we derive the closed-form expressions of MMSE and RD function for the scenario of TRM estimation,

and reformulate the original problem as a non-convex optimization task with reverse water-filling constraints. We then propose two distinct waveform design schemes that are widely considered in ISAC systems, namely, the separated S&C waveforms (SW) and dual-functional waveform (DW) designs.

- Third, for the SW design, we simplify the original matrix-valued optimization problem into a single scalar power allocation problem. Subsequently, a one-dimensional search algorithm is proposed to obtain the optimal solution, which implies a *power allocation tradeoff* between S&C waveform.
- Forth, for the DW design, we present a heuristic mutual information (MI) maximization algorithm for the general case, as well as a modified gradient projection algorithm for the case of independent sensing sub-channels. By doing so, we highlight the presence of both *subspace tradeoff* and *water-filling tradeoff* in this scenario.
- Finally, we validate the effectiveness of the proposed algorithms and analyze the performance tradeoffs by numerical results.

This paper is structured as follows. We commence with an introduction to the essential concepts of lossy data transmission, encompassing the RD and SCT theories. Additionally, we also introduce the well-studied optimal structures for MI-optimal communication waveform and the MMSE-optimal sensing waveform in Section II. In Section III, we establish a comprehensive CAS framework and formulate the optimization problem for the waveform design within such systems. We then present the corresponding waveform design algorithms for two typical signaling strategies, the SW in Section IV and the DW in Section V, respectively. In Section VI, we briefly discuss the design insights revealed from the development of the CAS system. The simulation results and the tradeoff analysis for the S&C performance are provided in Section VII. Finally, we conclude this paper in Section VIII.

## II. PRELIMINARIES

Lossy data transmission theory plays a vital role in characterizing the relationship between the distortion, coding rate, and channel capacity. Before elaborating on the CAS system design, we briefly introduce the contents of the RD and SCT, as well as the structures of MMSE-optimal sensing waveform and MI-optimal communication waveform. In this section, we use the uppercase normal letter  $A$ , lowercase italic letter  $a$ , and fraktur letter  $\mathcal{A}$  to represent a random variable, its realization, and a set, respectively.

### A. Lossy Data Transmission

1) *Rate-distortion Theory*: While using discrete codewords to represent a continuous random variable, *distortion* is defined to measure the distance between the random variable and its representation, evaluating the “goodness” of a representation. Let us denote  $A^N$  as an  $N$ -length sequence  $A_1, A_2, \dots, A_N$  independently and identically distributed (i.i.d.) with probability density function  $p_A(a)$ ,  $a \in \mathcal{A}$ . For a given coding rate  $R$ , a  $(2^{NR}, N)$  code that quantizes  $A^N$  consists of

- A encoder  $f_N : \mathcal{A}^N \rightarrow \{1, 2, \dots, 2^{NR}\}$ , mapping the source alphabet to an index set.
- A decoder  $g_N : \{1, 2, \dots, 2^{NR}\} \rightarrow \hat{\mathcal{A}}^N$ , reproducing the estimate  $\hat{A}^N$  from the index set.

Thus, the distortion associated with the  $(2^{NR}, N)$  code is defined by

$$D = \mathbb{E}[d(A^N, g_N(f_N(A^N)))], \quad (1)$$

where  $d : \mathcal{A}^N \times \hat{\mathcal{A}}^N \rightarrow \mathbb{R}^+$  is a distance metric (e.g., Hamming distortion, squared-error distortion) defined in terms of the specific requirements.

The RD theory characterizes the minimum information rate required to achieve a preset distortion, or equivalently, the minimum distortion achievable at a particular rate. For a given source distribution  $p_A(a)$  and distance metric  $d$ , the rate-distortion function  $R(D)$  and its inverse  $D(R)$  functions are defined by [20]

$$\begin{aligned} R(D) &= \min_{p_{\hat{A}|A} : \mathbb{E}[d(A, \hat{A})] \leq D} I(A; \hat{A}), \\ D(R) &= \min_{p_{\hat{A}|A} : I(A; \hat{A}) \leq R} \mathbb{E}[d(A, \hat{A})], \end{aligned} \quad (2)$$

where  $I(A; \hat{A})$  represents the MI between the source and its representation. It is worth pointing out that both  $R(D)$  and  $D(R)$  are the *monotonic non-increasing convex* functions, cf. [20, Lemma 10.4.1].

#### 2) Source-Channel Separation Theorem with Distortion:

Essentially, the communication process may be generally treated as that the encoded source passes through a noisy channel, where the distortion achieved at the receiving end depends on both the lossy source coding rate and the channel capacity. The SCT with distortion demonstrates the fact that a lossy source code with a rate  $R(D)$ , can be recovered with distortion  $D$  after passing through a channel with capacity  $C$ , if and only if [20]

$$R(D) < C. \quad (3)$$

3) *Quadratic Gaussian Problem*: In general, it is a challenging task to derive the explicit expression of the RD function in (2) with an arbitrary source distribution and distance metric. For analysis convenience, we focus on the *quadratic Gaussian problem* where the squared-error distortion is adopted in the scenario of Gaussian sources [28]. Specifically, for  $A_i \sim \mathcal{CN}(0, \lambda_i)$ ,  $i = 1, 2, \dots, N$ , the squared-error measure can be expressed by

$$d(a^N, \hat{a}^N) = \sum_{i=1}^N (a_i - \hat{a}_i)^2. \quad (4)$$

Thus, the corresponding distortion  $\mathbb{E}[d(A; \hat{A})]$  is the mean squared error (MSE). In such a case, the explicit expression of RD function can be given by [20, Th. 10.3.3]<sup>1</sup>

$$R(D) = \sum_{i=1}^N \log \frac{\lambda_i}{D_i}. \quad (5)$$

<sup>1</sup>The coefficient  $\frac{1}{2}$  vanishes since complex variables are considered.

The distortion  $D_i$  may be given in a reverse water-filling form as

$$\sum_{i=1}^N D_i = D, \quad D_i = \begin{cases} \xi, & \text{if } \xi < \lambda_i, \\ \lambda_i, & \text{if } \xi \geq \lambda_i. \end{cases} \quad (6)$$

where  $\xi$  represents the reverse water-filling factor. Eq. 6 is also equivalent to a compact form as  $D_i = \lambda_i - (\lambda_i - \xi)^+$ .

### B. Optimal Structures of S&C Waveforms

For decades, S&C researchers have been mostly working on the general Gaussian linear model as follows

$$\mathbf{Y} = \mathbf{H}\mathbf{X} + \mathbf{Z}, \quad (7)$$

where  $\mathbf{Y} \in \mathbb{C}^{M \times T}$ ,  $\mathbf{X} \in \mathbb{C}^{N \times T}$ , and  $\mathbf{Z} \in \mathbb{C}^{M \times T}$  are the received signal, transmitted signal, and additive Gaussian noise, respectively.  $\mathbf{H} \in \mathbb{C}^{M \times N}$  represents the transmission channel that is known in the communication system but to be estimated in the sensing systems.  $T$ ,  $N$ , and  $M$  are the numbers of symbols, transmitting and receiving antennas at the BS, respectively. We assume that the entries of  $\mathbf{Z}$  follow the complex Gaussian distribution with  $\mathcal{CN}(0, \sigma^2)$ .

The purpose of S&C waveform design is to find an appropriate transmission strategy  $\mathbf{X}$  to optimize the performance based on some criteria while satisfying the power budget. In what follows, we will introduce two well-studied waveform design schemes and the structures of optimal solutions  $\mathbf{X}^*$  for S&C systems, which will be differentiated by the subscripts  $s$  and  $c$ , respectively.

1) *MI-Optimal Communication Waveform*: For communication systems, the transmitted waveform  $\mathbf{X}_c$  is a random signal unknown at the receiver. With the Gaussian signal  $\mathbf{X}_c \sim \mathcal{CN}(\mathbf{0}, \mathbf{R}_c)$ , the MI between the received and transmitted signals conditioned on communication channel  $\mathbf{H}_c$  can be characterized by

$$I(\mathbf{Y}_c; \mathbf{X}_c | \mathbf{H}_c) = \log \left| \frac{1}{\sigma_c^2} \mathbf{H}_c \mathbf{R}_c \mathbf{H}_c^H + \mathbf{I}_N \right| \triangleq I_c(\mathbf{R}_c). \quad (8)$$

where  $\mathbf{R}_c \in \mathbb{C}^{N \times N}$  is the statistical covariance matrix, and the channel  $\mathbf{H}_c$  is assumed to be perfectly known. The MI-optimal waveform design problem may be formulated as

$$\max_{\mathbf{R}_c} I_c(\mathbf{R}_c), \quad \text{s.t. } \text{Tr}(\mathbf{R}_c) \leq P_T, \quad (9)$$

where  $P_T$  is the total power budget. The global optimal solution  $\mathbf{R}_c^*$  can be readily obtained since problem (9) is convex with respect to (w.r.t.)  $\mathbf{R}_c$ . Then, the optimal waveform  $\mathbf{X}_c^*$  may be reconstructed according to the covariance matrix  $\mathbf{R}_c^*$ , yielding

$$\mathbf{X}_c^* = \mathbf{\Psi}_c \mathbf{\Lambda}_c \mathbf{Q}_c^H, \quad (10)$$

where  $\mathbf{\Lambda}_c$  is a diagonal matrix with the eigenvalues of  $\mathbf{R}_c^*$  as its diagonal entries, the columns of  $\mathbf{\Psi}_c$  are the corresponding eigenvectors, and  $\mathbf{Q}_c$  contains i.i.d. circularly symmetric complex entries satisfying  $\mathbb{E}[\mathbf{Q}_c \mathbf{Q}_c^H] = \mathbf{I}_N$ . Furthermore, it is worth highlighting that the specific structure of  $\mathbf{X}_c^*$  admits  $\mathbf{\Psi}_c = \mathbf{U}_c$ , and

$$\mathbf{\Lambda}_c = \left( \text{diag} \left[ \left( \zeta_c - \frac{\sigma_c^2}{\lambda_{c1}} \right)^+, \dots, \left( \zeta_c - \frac{\sigma_c^2}{\lambda_{cN}} \right)^+ \right] \right)^{\frac{1}{2}}, \quad (11)$$

where  $\lambda_{c_i} \geq 0$  and  $\mathbf{U}_c$  are the eigenvalues and the eigenspace of the positive semidefinite matrix  $\mathbf{\Sigma}_c = \mathbf{H}_c^H \mathbf{H}_c$ , respectively, and  $\zeta_c$  is the water-filling factor such that  $\sum_{i=1}^N (\zeta_c - \sigma_c^2 / \lambda_{c_i})^+ = P_T$ .

2) *MMSE-Optimal Sensing Waveform*: The sensing task is to estimate  $\mathbf{H}_s$ , or, more relevant to radar sensing, to estimate the target parameters (e.g., amplitude, delay, angle, and Doppler) contained in  $\mathbf{H}_s$  as accurate as possible. Next, we introduce the optimal waveform design for the MMSE-based target response matrix (TRM) estimation. By vectorizing the Hermitian of the received signal in (7), we have

$$\mathbf{y}_s = \tilde{\mathbf{X}}_s \mathbf{h}_s + \mathbf{z}_s, \quad (12)$$

where  $\mathbf{y}_s = \text{vec}(\mathbf{Y}_s^H)$ ,  $\tilde{\mathbf{X}}_s = \mathbf{I}_{M_s} \otimes \mathbf{X}_s^H$ ,  $\mathbf{h}_s = \text{vec}(\mathbf{H}_s^H)$ ,  $\mathbf{z}_s = \text{vec}(\mathbf{Z}_s^H)$ . TRM estimation is to obtain the  $\mathbf{h}_s$  from noisy received signal  $\mathbf{y}_s$ . Here, we make the following assumptions on the parameter's prior distribution:

**Assumption 1.** The random vector  $\mathbf{h}_s$  follows complex Gaussian distribution  $\mathcal{CN}(0, \mathbf{I}_{M_s} \otimes \mathbf{\Sigma}_s)$  with  $\mathbf{\Sigma}_s \in \mathbb{C}^{N \times N}$  being the covariance matrix of each column of  $\mathbf{H}_s$ . This corresponds to the scenario that the receiving antennas for sensing are sufficiently separated so that the correlations among the rows of  $\mathbf{H}_s$  can be ignored [29].

Under the Assumption 1, the MMSE between  $\mathbf{h}_s$  and its estimate  $\hat{\mathbf{h}}_s$  may be expressed by

$$\mathbb{E}[\|\mathbf{h}_s - \hat{\mathbf{h}}_s\|^2] = M_s \text{Tr} \left[ \left( \frac{1}{\sigma_s^2} \mathbf{X}_s \mathbf{X}_s^H + \mathbf{\Sigma}_s^{-1} \right)^{-1} \right]. \quad (13)$$

By denoting  $\mathbf{R}_s = 1/T \mathbf{X}_s \mathbf{X}_s^H$  as the sample covariance matrix, the MMSE-optimal waveform design may be formulated by a convex problem w.r.t.  $\mathbf{R}_s$ , i.e.,

$$\min_{\mathbf{R}_s} \text{MMSE}(\mathbf{R}_s), \quad \text{s.t. } \text{Tr}(\mathbf{R}_s) \leq P_T. \quad (14)$$

Similarly, by denoting the eigenvalue decomposition of  $\mathbf{R}_s^* = \mathbf{\Psi}_s \mathbf{\Lambda}_s \mathbf{\Psi}_s^H$ , the optimal waveform  $\mathbf{X}_s^*$  may be reconstructed by

$$\mathbf{X}_s^* = \mathbf{\Psi}_s \mathbf{\Lambda}_s \mathbf{Q}_s^H, \quad (15)$$

which also yields the following specific structure [30]

$$\mathbf{X}_s^* = \mathbf{U}_s \left( \text{diag} \left[ \left( \zeta_s - \frac{\sigma_s^2}{\lambda_{s1}} \right)^+, \dots, \left( \zeta_s - \frac{\sigma_s^2}{\lambda_{sN}} \right)^+ \right] \right)^{\frac{1}{2}} \mathbf{Q}_s^H, \quad (16)$$

where  $\lambda_{s_i} \geq 0$  and  $\mathbf{U}_s$  are the eigenvalues and the corresponding eigenspace of matrix  $\mathbf{\Sigma}_s$ , respectively.  $\mathbf{Q}_s$  is an arbitrary semi-unitary matrix, and  $\zeta_s$  represents the water filling factor. The detailed derivations can be found in [30].

**Remark 1:** From the specific structures of the S&C waveforms, one may observe that the random matrix  $\mathbf{Q}_c$  and semi-unitary matrix  $\mathbf{Q}_s$  are flexibly designed in terms of the symbol level requirements. Consequently, the MI- and MMSE-optimal waveform designs (9) and (14) may only determine the left singular matrices  $\mathbf{\Psi}_c$  and  $\mathbf{\Psi}_s$ , and the water-filling type power allocation strategies  $\mathbf{\Lambda}_s$  and  $\mathbf{\Lambda}_c$ . Consequently, we rewrite the MI and MMSE as the following form

$$I_c(\mathbf{\Psi}_c, \mathbf{\Lambda}_c) = \log \left| \frac{1}{\sigma_c^2} \mathbf{H}_c \mathbf{\Psi}_c \mathbf{\Lambda}_c^2 \mathbf{\Psi}_c^H \mathbf{H}_c^H + \mathbf{I}_N \right|, \quad (17a)$$

$$D_s(\mathbf{\Psi}_s, \mathbf{\Lambda}_s) = M_s \text{Tr} \left[ \left( \frac{1}{\sigma_s^2} \mathbf{\Psi}_s \mathbf{\Lambda}_s^2 \mathbf{\Psi}_s^H + \mathbf{\Sigma}_s^{-1} \right)^{-1} \right]. \quad (17b)$$

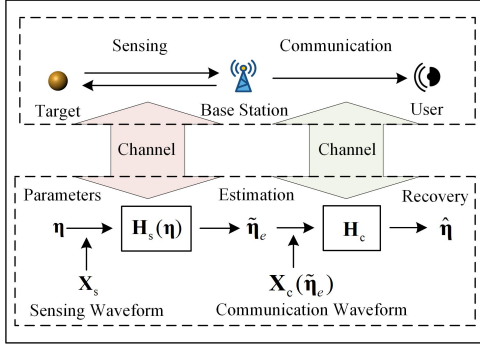


Fig. 2. The to-be-estimated parameters successively “pass through” the S&C channels to the user.

### III. THE CAS FRAMEWORK

In this section, we establish the CAS framework based on the RD and SCT theorems. The EC scheme is adopted where the BS transmits the estimates of the parameters rather than the raw data to the end-user. Then, we formulate a general waveform design problem within the CAS framework and derive the explicit expressions of the MMSE and RD function in the scenario of TRM estimation.

#### A. System Model and Problem Formulation

Let us consider a BS equipped with  $N$  transmitting and  $M_s$  receiving antennas, which senses a point-like target, and then delivers the parameter estimation information to an  $M_c$ -antenna user. Denote  $\eta \in \mathbb{R}^K$  as the parameter vector to be sensed, which takes the value on a set  $\mathcal{A}$  with a prior distribution  $p_\eta(\eta)$ . As shown in Fig. 2, the CAS process can be equivalently regarded as that the target information successively “passes through” the S&C channels before its arrival at the user. In such a case, the original parameter  $\eta$ , the estimated  $\tilde{\eta}_e$  at the BS, and the recovered  $\hat{\eta}$  at the user forms a Markov chain  $\eta \rightarrow \tilde{\eta}_e \rightarrow \hat{\eta}$ . The detailed signal models are as follows.

- **Sensing side (S-side):** The BS transmits sensing waveform to the target and yields the estimated parameter, namely,  $\tilde{\eta}_e$  through the noisy echo signals. Similar to (7), the received signal model can be expressed by

$$\mathbf{Y}_s = \mathbf{H}_s(\eta)\mathbf{X}_s + \mathbf{Z}_s, \quad (18)$$

where  $\mathbf{H}_s(\eta)$  represents the sensing channel matrix w.r.t. the latent parameters  $\eta$ .

- **Communication side (C-side):** The estimated information  $\tilde{\eta}_e$  is transmitted to the user, then be reconstructed as an estimate  $\hat{\eta}$  from the following received signal

$$\mathbf{Y}_c = \mathbf{H}_c\mathbf{X}_c(\tilde{\eta}_e) + \mathbf{Z}_c. \quad (19)$$

Here, we use  $\mathbf{X}_c(\tilde{\eta}_e)$  to emphasize the waveform carrying the information of  $\tilde{\eta}_e$  through source-channel coding.

Here, we adopt the classical MSE between the recovery  $\hat{\eta}$  and the ground truth  $\eta$  as the distortion metric. In the CAS system, the sensing QoS is defined by the average distortion between the recoveries at the user and the ground truths, i.e.,

$$D = \mathbb{E}[\|\eta - \hat{\eta}\|_2^2]. \quad (20)$$

We can observe that the achievable  $D$  depends on both the estimation distortion  $D_s$  at S-side and the recovery distortion  $D_c$  at C-side. Furthermore, the estimation distortion  $D_s$  is directly determined by the sensing waveform  $\mathbf{X}_s$ . On the other hand, as demonstrated by the SCT in Section II-A, the minimum achievable recovery distortion  $D_c$  is bounded by the achievable rate  $I_c$ , relying on the communication waveform  $\mathbf{X}_c$ . This motivates us to design the optimal waveform such that the distortion  $D$  is minimized, where the optimization problem can be formulated as <sup>2</sup>

$$\mathcal{P}_0 \begin{cases} \min_{\mathbf{X}_s, \mathbf{X}_c} D \\ \text{subject to } R(D_c) \leq I_c, \\ \text{Tr}(\mathbf{X}_s\mathbf{X}_s^H) + \text{Tr}(\mathbf{X}_c\mathbf{X}_c^H) \leq P_T, \end{cases} \quad (21)$$

In the above concise form, the to-be-optimized variables  $\mathbf{X}_s$  and  $\mathbf{X}_c$  are implicit in the objective and SCT constraint. In what follows, to clearly reveal the performance tradeoffs between S&C subsystems and bring insights into the CAS waveform design, we will focus on the specified sensing TRM estimation and leave the more general target motion parameter estimation for future research.

#### B. Target Response Matrix Estimation

For TRM estimation, the to-be-estimated parameter is the sensing channel matrix itself, i.e.,  $\eta = \mathbf{h}_s$ . Under the Assumption 1, the received signal (12) becomes a Gaussian linear model and MMSE is known as the optimal linear estimator. Next, we will derive the explicit expressions of the MMSE and RD function in  $\mathcal{P}_0$  for the considered scenario.

1) **Objective Function:** The distortion  $D$  can be equivalently decomposed into the sum of the estimation distortion  $D_s$  and the recovery distortion  $D_c$  <sup>3</sup>, i.e.,

$$\begin{aligned} D_{sc} &= \mathbb{E}[\|\eta - \tilde{\eta}_e + \tilde{\eta}_e - \hat{\eta}\|_2^2] \\ &\stackrel{(a)}{=} \mathbb{E}[\|\eta - \tilde{\eta}_e\|_2^2] + \mathbb{E}[\|\tilde{\eta}_e - \hat{\eta}\|_2^2] \triangleq D_s + D_c, \end{aligned} \quad (22)$$

where (a) holds due to the conditional expectation

$$\mathbb{E}[(\eta - \tilde{\eta}_e)^T(\tilde{\eta}_e - \hat{\eta})] = \mathbb{E}[(\eta - \mathbb{E}[\eta|\mathbf{y}_s])^T\phi(\mathbf{y}_s)] = 0.$$

Here,  $\tilde{\eta}_e = \mathbb{E}[\eta|\mathbf{y}_s]$  is the MMSE estimator, and  $\phi(\mathbf{y}_s)$  represents an arbitrary function w.r.t.  $\mathbf{y}_s$  [28].

2) **Estimate  $\tilde{\eta}_e$  and Distortion  $D_s$ :** The observations  $\mathbf{y}_s$  follows complex Gaussian distribution  $\mathcal{CN}(\mathbf{0}, \tilde{\mathbf{R}}_y)$ , with the covariance matrix of

$$\tilde{\mathbf{R}}_y = \mathbf{I}_{M_s} \otimes (\mathbf{X}_s^H \Sigma_s \mathbf{X}_s + \sigma_s^2 \mathbf{I}_T) \triangleq \mathbf{I}_{M_s} \otimes \mathbf{R}_y, \quad (23)$$

where  $\mathbf{R}_y \triangleq \mathbf{X}_s^H \Sigma_s \mathbf{X}_s + \sigma_s^2 \mathbf{I}_T$ . In this case, the MMSE estimate  $\tilde{\eta}_e$  can be expressed by [31]

$$\tilde{\eta}_e = \left( \mathbf{I}_{M_s} \otimes (\Sigma_s \mathbf{X}_s \mathbf{R}_y^{-1}) \right) \mathbf{y}_s, \quad (24)$$

<sup>2</sup>Here, we slightly modify the SCT constraint by transforming the strict “<” of (3) into “≤”. On one hand, this modification can significantly simplify the analysis and solution of the optimization problem. On the other hand, different from the information theory, the error caused by this operation is tolerable in practical applications.

<sup>3</sup>This equality holds since we adopt MSE as the distortion metric and MMSE as the estimator. This decomposition may not be applicable to a general case.

which also follows complex Gaussian distribution  $\mathcal{CN}(\mathbf{0}, \tilde{\mathbf{R}}_\eta)$ , with the covariance matrix of

$$\tilde{\mathbf{R}}_\eta = \mathbf{I}_{M_s} \otimes \Sigma_s \mathbf{X}_s \mathbf{R}_y^{-1} \mathbf{X}_s^H \Sigma_s^H \triangleq \mathbf{I}_{M_s} \otimes \mathbf{R}_\eta. \quad (25)$$

Here, by applying the waveform structure (15), the matrix  $\mathbf{R}_\eta$  can be recast by

$$\mathbf{R}_\eta \triangleq \Sigma_s \Psi_s \Lambda_s \left( \Lambda_s \Psi_s^H \Sigma_s \Psi_s \Lambda_s + \sigma_s^2 \mathbf{I}_T \right)^{-1} \Lambda_s \Psi_s^H \Sigma_s^H, \quad (26)$$

which is related to  $\Psi_s$  and  $\Lambda_s$ . Meanwhile, the sensing distortion  $D_s$  is achieved by the MMSE given in (17b).

3) *Recovery Distortion  $D_c$* : The purpose at C-side is to transmit the Gaussian random variables  $\tilde{\eta}_e$  to the user through source-channel coding. Note that unitary rotation would not cause any information loss in Gaussian variables. Let us denote  $\tilde{\eta}_s = \mathbf{U}_\eta^H \tilde{\eta}_e$ , where  $\mathbf{U}_\eta$  is the eigenspace of matrix  $\mathbf{R}_\eta$ . Thus, we have

$$\tilde{\eta}_s \sim \mathcal{CN}(\mathbf{0}, \mathbf{I}_{M_s} \otimes \text{diag}[\lambda_1(\mathbf{R}_\eta), \dots, \lambda_N(\mathbf{R}_\eta)]), \quad (27)$$

where  $\lambda_i(\mathbf{R}_\eta)$  represents the  $i$ -th eigenvalue of matrix  $\mathbf{R}_\eta$ . Based on the results in Section II-A3, the RD function can be obtained by

$$R(D_c) = M_s \sum_{i=1}^N \log \frac{\lambda_i(\mathbf{R}_\eta)}{D_{c_i}}, \quad (28)$$

which is in a reverse water-filling form as

$$D_c = M_s \sum_{i=1}^N D_{c_i} = M_s \sum_{i=1}^N \lambda_i(\mathbf{R}_\eta) - (\lambda_i(\mathbf{R}_\eta) - \xi)^+. \quad (29)$$

With the achievable rate  $I_c(\Psi_c, \Lambda_c)$  given in (17a), the original problem  $\mathcal{P}_0$  can be transformed into the following form in the scenario of TRM estimation,

$$\mathcal{P}_1 \begin{cases} \min_{\Psi_c, \Psi_s, \Lambda_c, \Lambda_s} D_s(\Psi_s, \Lambda_s) + D_c \\ \text{s.t.} \quad M_s \sum_{i=1}^N \log \frac{\lambda_i(\mathbf{R}_\eta)}{D_{c_i}} \leq I_c(\Psi_c, \Lambda_c), \\ 29, \text{Tr}(\Lambda_c^2) + \text{Tr}(\Lambda_s^2) \leq P_T. \end{cases} \quad (30)$$

Apparently, addressing the non-convex problem  $\mathcal{P}_1$  presents inherent challenges due to two primary reasons: 1) The eigenvalue  $\lambda_i(\mathbf{R}_\eta)$  of matrix  $\mathbf{R}_\eta$  is still an implicit function w.r.t. the variables  $\Psi_s$  and  $\Lambda_s$ . 2) The imposed reverse water-filling constraint introduces an unknown nuisance parameter (i.e., the factor  $\xi$ ), which may only be determined through a numerical search algorithm in general. In what follows, we will propose waveform design approaches for two typical signaling schemes within the ISAC system, i.e., the SW and DW designs. Furthermore, we will reveal the inherent tradeoffs in performance between S-side and C-side.

#### IV. SEPARATED S&C WAVEFORM DESIGN

In the SW strategy, the BS transmits individual waveforms at S-side and C-side by the shared use of the transmission power. By recalling the optimal waveform structures in Section II-B, this implies that the eigenspaces of SW may be independently designed but the diagonal power allocation

matrices are coupled through the power budget constraint. For discussion convenience, we refer the eigenspaces  $\mathbf{U}_s$  and  $\mathbf{U}_c$  of the matrices  $\Sigma_s$  and  $\Sigma_c$  to as *sensing subspace* and *communication subspace*, respectively. Let the left singular spaces of S&C waveforms align with the S&C subspaces, respectively, i.e.,  $\Psi_s = \mathbf{U}_s$  and  $\Psi_c = \mathbf{U}_c$ , and denote

$$\Lambda_s = \text{diag}[\sqrt{\mathbf{p}_s}], \quad \Lambda_c = \text{diag}[\sqrt{\mathbf{p}_c}], \quad (31)$$

where  $\mathbf{p}_s = [p_{s_1}, \dots, p_{s_N}]^T$  and  $\mathbf{p}_c = [p_{c_1}, \dots, p_{c_N}]^T$  represent the power allocation vectors. Then, we have

$$I_c(\Lambda_c) = I_c(\mathbf{p}_c) = \sum_{i=1}^N \log \left( \frac{\lambda_{c_i}}{\sigma_c^2} p_{c_i} + 1 \right), \quad (32a)$$

$$D_s(\Lambda_s) = D_s(\mathbf{p}_s) = M_s \sum_{i=1}^N \frac{\lambda_{s_i} \sigma_s^2}{\sigma_s^2 + \lambda_{s_i} p_{s_i}}, \quad (32b)$$

$$\lambda_i(\mathbf{R}_\eta) = \frac{\lambda_{s_i}^2 p_{s_i}}{\sigma_s^2 + \lambda_{s_i} p_{s_i}} \triangleq s_i(p_{s_i}), \quad (32c)$$

By applying the optimal subspace alignment, the eigenvalue  $\lambda_i(\mathbf{R}_\eta)$  can be explicitly expressed by the function of the variable  $p_{s_i}$ , denoted by  $s_i(p_{s_i})$ , thereby circumventing the eigenvalue decomposition. Let us define the MMSE of the  $i$ -th subchannel in (32b) as  $f_i(p_{s_i}) \triangleq \frac{\lambda_{s_i} \sigma_s^2}{\sigma_s^2 + \lambda_{s_i} p_{s_i}}$ . Thus, we have

$$s_i(p_{s_i}) = \lambda_{s_i} - f_i(p_{s_i}), \forall i = 1, 2, \dots, N. \quad (33)$$

Eq. (33) suggests that the source variances at C-side are equal to the prior variances of the parameters minus the MMSE achieved at S-side. Consequently, the original problem  $\mathcal{P}_1$  with  $N \times N$ -dimension matrix variables can be simplified into  $N$ -dimension vector variables, given by

$$\mathcal{P}_2 \begin{cases} \min_{\mathbf{p}_s, \mathbf{p}_c} M_s \sum_{i=1}^N (\lambda_{s_i} - (s_i(p_{s_i}) - \xi)^+) \\ \text{s.t.} \quad M_s \sum_{i=1}^N \log \frac{s_i(p_{s_i})}{s_i(p_{s_i}) - (s_i(p_{s_i}) - \xi)^+} \leq I_c(\mathbf{p}_c), \\ \mathbf{1}_N^T (\mathbf{p}_s + \mathbf{p}_c) \leq P_T, \quad \mathbf{p}_s, \mathbf{p}_c \geq 0. \end{cases} \quad (34)$$

Problem  $\mathcal{P}_2$  is exactly a power allocation problem, which aims at minimizing the total distortion under the constraints of SCT and power budget. Before solving  $\mathcal{P}_2$ , we first show that both constraints are active at the optimal solution.

**Proposition 1:** The optimal solutions  $\mathbf{p}_s^*$  and  $\mathbf{p}_c^*$  are achieved if and only if the equality holds in both the SCT and power budget constraints.

**Proof:** Please see Appendix A. ■

#### A. A General One-Dimensional Search Algorithm

Let us denote  $P_s$  and  $P_c$  as the total power allocated to the S-side and C-side, satisfying  $P_s + P_c = P_T$ . According to Proposition 1, we will show that the solution  $(\mathbf{p}_s^*, \mathbf{p}_c^*)$  is uniquely determined once the power allocation pair  $(P_s, P_c)$  is given. This implies that we can just search the optimal power allocation pair  $(P_s, P_c)$  instead of solving problem  $\mathcal{P}_2$  directly.



---

**Algorithm 1:** One-dimensional search algorithm

---

```

1 Initialize: Grid number  $L$ , power budget  $P_T$ ,  $\epsilon > 0$ .
2  $p_{\min} = 0$ ,  $p_{\max} = P_T$ ;
3 while  $|D^{(k+1)} - D^{(k)}| > \epsilon$  do
4   for  $l = 0 : L$  do
5      $P_{s,l} = p_{\min} + \frac{l}{L}(p_{\max} - p_{\min})$ ,  $P_{c,l} = P_T - P_{s,l}$ ;
6     Obtain  $\mathbf{p}_{c,l}$  in (35), then calculate  $I_{c,l}$  in (32a);
7     Obtain  $\mathbf{p}_{s,l}$  in (36), then calculate  $D_{s,l}$  and  $s_{i,l}$ 
       in (32b) and (32c), respectively;
8     Calculate  $D_{c,l}$  by reverse water-filling in (6);
9      $D^{(k)} \leftarrow D_l = D_{s,l} + D_{c,l}$ ;
10  end
11   $D^{(k+1)} \leftarrow \min D \in \mathcal{D}^{(k)}$ ,  $l^*$  is the grid index;
12   $p_{\min} = P_{s,l^*-1}$ ,  $p_{\max} = P_{s,l^*+1}$ ;
13 end
Output:  $(\mathbf{p}_s^*, \mathbf{p}_c^*)$  for  $D^*$ .

```

---

1) *Maximizing Achievable Rate:* The power  $P_c$  allocated to the C-side only affects on the achievable rate in problem  $\mathcal{P}_2$ . As previously discussed, the optimal solution  $\mathbf{p}_c^*$  of maximizing the achievable rate can be expressed by

$$p_{c_i} = \left( \zeta_c - \frac{\sigma_c^2}{\lambda_{c_i}} \right)^+, \quad \sum_{i=1}^N p_{c_i} = P_c. \quad (35)$$

2) *Minimizing Sensing Distortion:* Similarly, for a given power  $P_s$ , the minimum sensing distortion can be attained by the following solution

$$p_{s_i} = \left( \zeta_s - \frac{\sigma_s^2}{\lambda_{s_i}} \right)^+, \quad \sum_{i=1}^N p_{s_i} = P_s. \quad (36)$$

3) *Calculating Recovery Distortion:* With the power allocation  $\mathbf{p}_s^*$  in 36 at hand, we can immediately compute the source variance  $s_i$  through (33). At the same time, the maximum available coding rate, i.e.,  $R = I_c$  is determined. Therefore, the recovery distortion  $D_c$  can be obtained through the reverse water-filling algorithm in (6), thereby the total distortion  $D$ .

Following the above steps, we may identify the optimal solution  $(\mathbf{p}_s^*, \mathbf{p}_c^*)$  and the objective value with a given power allocation pair  $(P_s, P_c)$ . The remaining work is to find optimal  $(P_s^*, P_c^*)$  with the constraint of total power  $P_T$ . Consequently, we develop the idea of bisection search to seek for the optimal solution of  $\mathcal{P}_2$  over the discrete grid points  $P_s \in [0, P_T]$ ,  $P_c = P_T - P_s$ . The detailed algorithm flow is summarized in Algorithm 1.

### B. Special Case: I.I.D. Sensing Subchannels

To further reveal the tradeoff between S-side and C-side, in this subsection, we focus on a special case that the entries of TRM are i.i.d. white Gaussian distributed, namely,

**Assumption 2:** The vector  $\mathbf{h}_s$  follows  $\mathcal{CN}(0, \lambda_s \mathbf{I}_{M_s N})$ .

In this scenario, one may readily attain the following results.

- The optimal  $\mathbf{p}_s^*$  is the uniform power allocation with  $p_{s_1} = \dots = p_{s_N} = P_s/N$ . This leads to the identical

values of the sensing distortion and source variance for each subchannel, denoted by

$$f(P_s) = \frac{N\lambda_s\sigma_s^2}{N\sigma_s^2 + \lambda_s P_s}, \quad s(P_s) = \frac{\lambda_s^2 P_s}{N\sigma_s^2 + \lambda_s P_s}. \quad (37)$$

- Note that  $s(P_s) - \xi > 0$  always holds with a positive achievable rate  $I_c$ . Consequently, the recovery distortion can be expressed by  $D_{c_i} = s(P_s) - (s(P_s) - \xi)^+ = \xi$ . Thus, the SCT constraint at the optimal point is recast by

$$M_s N \log \frac{s(P_s)}{\xi} = I_c(P_T - P_s). \quad (38)$$

Fortunately, we can obtain the expression of the water-filling factor  $\xi$  from 38 instead of the numerical searching. By substituting  $\xi$  into the objective, problem  $\mathcal{P}_2$  may be further reformulated as an unconstrained optimization problem w.r.t. the scalar variable  $P_s$ , namely,

$$\mathcal{P}_3 : \min_{P_s} N M_s \left[ \left( 1 - e^{-\frac{I_c(P_T - P_s)}{M_s N}} \right) f(P_s) + \lambda_s e^{-\frac{I_c(P_T - P_s)}{M_s N}} \right]. \quad (39)$$

**Proposition 2:**  $\mathcal{P}_3$  is a convex optimization problem.

**Proof:** Please see Appendix B. ■

**Remark 2:** Problem  $\mathcal{P}_3$  clearly shows the tradeoff between S-side and C-side. Let us denote the objective of  $\mathcal{P}_3$  as  $h(x)$ . Then it holds immediately that  $h(0) = h(P_T) = \lambda_s$ . The physical meanings involve that no useful information will be attained by the user if the total power is allocated to either S-side or C-side. In this case, the user may only “guess” the target parameters with the prior knowledge of variance  $\lambda_s$ . Considering the convexity of  $\mathcal{P}_3$ , there exists an optimal power allocation scheme between  $[0, P_T]$ . This exhibits a *power allocation tradeoff* between S&C in the CAS systems, where extremely allocating resources to each side will lead to significant performance loss.

## V. DUAL-FUNCTIONAL WAVEFORM DESIGN

In this section, we consider that the DW, i.e.,  $\mathbf{X}_s = \mathbf{X}_c = \mathbf{X} = \mathbf{\Psi} \mathbf{\Lambda} \mathbf{Q}^H$ , is adopted to sense the targets and convey the estimates at the last epoch to the user simultaneously. In this scenario,  $\mathbf{Q}$  should be a random matrix to convey useful information. The system design which considers the randomness of  $\mathbf{Q}$  is beyond the scope of this paper. The readers are referred to [9], [32] for more details. Similar to problem  $\mathcal{P}_1$ , the DW design can be formulated by

$$\mathcal{P}_4 \begin{cases} \min_{\mathbf{\Psi}, \mathbf{\Lambda}} D_s(\mathbf{\Psi}, \mathbf{\Lambda}) + D_c \\ \text{s.t. } M_s \sum_{i=1}^N \log \frac{\lambda_i(\mathbf{R}_\eta)}{D_{c_i}} \leq I_c(\mathbf{\Psi}, \mathbf{\Lambda}), \\ 29, \text{Tr}(\mathbf{\Lambda}^2) \leq T P_T. \end{cases} \quad (40)$$

In addition to the challenges encountered when solving problem  $\mathcal{P}_3$ , the variables  $\mathbf{\Psi}, \mathbf{\Lambda}$  are coupled in both power budget and SCT constraints of problem  $\mathcal{P}_4$ . Therefore, the tradeoffs are manifested in the following two aspects.

- *Subspace tradeoff:* The left singular subspace  $\mathbf{\Psi}$  cannot align to the sensing subspace  $\mathbf{U}_s$  and the communication subspace  $\mathbf{U}_c$  simultaneously.

---

**Algorithm 2:** Heuristic MI maximization algorithm

---

1 **Initialize:** The grid number  $L$ .  
2 **for**  $l = 0 : L$  **do**  
3      $\alpha^{(l)} = l/L$ ;  
4     Solve problem (43) with  $\alpha^{(l)}$  and obtain  $\mathbf{R}^{(l)}$  ;  
5     Compute  $D_s(\mathbf{R}^{(l)})$  according to (13) ;  
6     Compute  $I_c(\mathbf{R}^{(l)})$  according to (8);  
7     Obtain  $\Psi^{(l)}, \Lambda^{(l)}$  according to  $\mathbf{R}^{(l)}$ ;  
8     Compute  $D_c(\Psi^{(l)}, \Lambda^{(l)})$  by reverse water-filling algorithm and  $\mathcal{D} \leftarrow D^{(l)} = D_s^{(l)} + D_c^{(l)}$ ;  
9 **end**  
   **Output:**  $\mathbf{R}^* = \arg \min_{\mathbf{D} \in \mathcal{D}} D(\mathbf{R})$ .

---

---

**Algorithm 3:** Modified gradient projection algorithm

---

1 **Initialize:** The initial point  $\mathbf{p}^{(0)} \in \mathcal{F}$ ,  $\alpha_1 > 0$ ,  $\epsilon > 0$ .  
2 **while**  $|h(\mathbf{p}^{(l+1)}) - h(\mathbf{p}^{(l)})| > \epsilon$  **do**  
3     Calculate  $K^{(l)}, \xi^{(l)}$  through reverse water-filling algorithm with given power vector  $\mathbf{p}^{(l)}$ ;  
4     Obtain the gradient  $\nabla h(\mathbf{p}^{(l)})$  by (49);  
5      $\tilde{\mathbf{p}}^{(l)} = \text{Proj}(\mathbf{p}^{(l)} + \alpha_1 \nabla h(\mathbf{p}^{(l)}))$ ;  
6     Find stepsize  $\alpha_2^{(l)}$  based on the Armijo condition;  
7      $\mathbf{p}^{(l+1)} = \mathbf{p}^{(l)} + \alpha_2^{(l)}(\tilde{\mathbf{p}}^{(l)} - \mathbf{p}^{(l)})$ ;  
8 **end**

---

- *Water-filling tradeoff:* Although the total transmit power is shared between S-side and C-side, the power allocation cannot satisfy the water-filling criteria of the sensing subchannel  $\sigma_s^2/\lambda_{s_i}$  and communication subchannel  $\sigma_c^2/\lambda_{c_i}$  simultaneously.

The above discussions illustrate that one cannot find a DW that simultaneously optimizes both S-side and C-side, unless the S&C channels are sufficiently similar.

#### A. A Heuristic MI Maximization Algorithm

Note that the optimal structures are no longer obtainable in the scenario of DW design due to the existence of a subspace tradeoff. Without a simplification process, solving the non-convex problem  $\mathcal{P}_4$  directly becomes a challenging task. This motivates us to transform the original problem into a more tractable MI maximization algorithm.

From the perspective of sensing waveform design, it is well known that minimizing MMSE has the same solution as maximizing the sensing MI between observations and TRM at the condition of  $\mathbf{X}$ , which can be written by [30]

$$I(\mathbf{Y}_s; \mathbf{H}_s | \mathbf{X}) = \log \left| \frac{1}{\sigma_s^2} \Sigma_s \mathbf{R} + \mathbf{I}_N \right| \triangleq I_s(\mathbf{R}), \quad (41)$$

where  $\mathbf{R}$  is the covariance matrix of signal  $\mathbf{X}$ . Recently, the authors of [33] have further shown that minimizing MMSE and maximizing MI is completely equivalent in the scenarios of quadratic Gaussian problem from the perspective of RD theory. Specifically, we have

$$R(D_s) = R(\text{MMSE}) = I(\mathbf{Y}_s; \mathbf{H}_s | \mathbf{X}), \quad (42)$$

by appropriately choosing the reverse water-filling factor as  $\xi_s = \sigma_s^2/\zeta_s$  [33]. Similarly, at the C-side, minimizing the distortion  $D_c$  is also equivalent to maximizing the achievable rate due to the SCT constraint  $R(D_c) = I_c$  by appropriately choosing to reverse water-filling factor  $\xi_c$ . Inspired by this observation, we transform the minimization of the sum of S&C distortions problem into a more tractable formulation that maximizes the sum of S&C MI. Unfortunately, the reverse water-filling factors are usually different between the two RD functions, i.e.,  $\xi_s \neq \xi_c$ , which implies that the equalities may not hold simultaneously in a high probability. To tackle this problem, we introduce a to-be-determined weighting factor  $\alpha$  to balance the S&C performance. Then, the weighted MI maximization problem can be formulated by

$$\begin{aligned} \max_{\mathbf{R}} \quad & \alpha I_s(\mathbf{R}) + (1 - \alpha) I_c(\mathbf{R}) \\ \text{s.t.} \quad & \text{Tr}(\mathbf{R}) \leq P_T. \end{aligned} \quad (43)$$

Problem (43) is convex since both MIs are concave w.r.t.  $\mathbf{R}$ . The optimal waveform  $\mathbf{X}$  may be immediately obtained by following the similar process in Section II. Furthermore, note that  $\alpha$  is a key parameter that determines the approximation performance between the original problem and the heuristic MI maximization problem. Therefore, we adopt a search procedure over the interval  $[0, 1]$  to seek for the optimal  $\alpha^*$ . The detailed algorithm flow is summarized in Algorithm 2.

#### B. Special Case: Independent Sensing Subchannel

In this subsection, we consider the following assumption.

**Assumption 3.**  $\mathbf{h}_s$  follows  $\mathcal{CN}(0, \mathbf{I}_{M_s} \otimes \Lambda_{h_s})$ , where  $\Lambda_{h_s}$  is a diagonal matrix with  $\Lambda_{h_s} = \text{diag}[\lambda_{s_1}, \lambda_{s_2}, \dots, \lambda_{s_N}]$ .

Under Assumption 3, the subspace tradeoff vanishes since sensing subspace  $\mathbf{U}_s$  can be an arbitrary unitary matrix. Let  $\Psi = \mathbf{U}_c$  and  $\Lambda = \text{diag}[\sqrt{p_1}, \sqrt{p_2}, \dots, \sqrt{p_N}]$ , the original problem can be transformed into the following form

$$\mathcal{P}_5 \left\{ \begin{aligned} & \min_{\mathbf{p}} M_s \sum_{i=1}^N (\lambda_s - (s_i(\mathbf{p}) - \xi)^+) \\ & \text{s.t. } M_s \sum_{i=1}^N \log \frac{s_i(\mathbf{p})}{s_i(\mathbf{p}) - (s_i(\mathbf{p}) - \xi)^+} \leq I_c(\mathbf{p}), \\ & \mathbf{1}_N^T \mathbf{p} \leq P_T, \mathbf{p} \geq 0. \end{aligned} \right. \quad (44)$$

where  $\mathbf{p} = [p_1, p_2, \dots, p_N]$ . Problem  $\mathcal{P}_5$  is still non-convex and the variable is coupled in both SCT and power constraints. To further simplify  $\mathcal{P}_5$ , we introduce an auxiliary variable  $K$  representing the number of the independent sources that contribute to the RD function. Namely, we have  $s_i(\mathbf{p}) \geq \xi, i = 1, 2, \dots, K$ . Thus,  $\mathcal{P}_5$  can be equivalently transformed into the following problem

$$\begin{aligned} \max_{\mathbf{p}, K} \quad & \sum_{i=1}^K s_i(\mathbf{p}) - K\xi \\ \text{s.t.} \quad & M_s \sum_{i=1}^K \log \frac{s_i(\mathbf{p})}{\xi} \leq I_c(\mathbf{p}), 0 < K \leq N, \\ & \mathbf{1}_N^T \mathbf{p} \leq P_T, \mathbf{p} \geq 0. \end{aligned} \quad (45)$$



Note that  $K$  can be immediately obtained through the reverse water-filling algorithm once the power vector  $\mathbf{p}$  is determined.

The SCT constraint is still active through a similar proof as in Appendix A. Therefore,  $\xi$  can be expressed through the equality constraint, which is

$$\xi = e^{g(\mathbf{p})}, g(\mathbf{p}) \triangleq \left[ \sum_{i=1}^K \log s_i(\mathbf{p}) - \frac{I_c(\mathbf{p})}{M_s} \right] / K. \quad (46)$$

For a fixed  $K$ , problem (45) can be transformed into

$$\max_{\mathbf{p} \in \mathcal{F}} h(\mathbf{p}) := \sum_{i=1}^K s_i(\mathbf{p}) - K e^{g(\mathbf{p})}, \quad (47)$$

where the feasible region is denoted by  $\mathcal{F} = \{\mathbf{p} | \mathbf{1}_N^T \mathbf{p} \leq P_T, \mathbf{p} \geq 0\}$ . Since  $\mathcal{F}$  is convex and the objective function is differentiable, we propose a gradient projection method to solve problem (47). Specifically, we have

$$\frac{\partial h(\mathbf{p})}{\partial p_i} = \frac{\lambda_{s_i}^2 \sigma_s^2}{(\sigma_s^2 + \lambda_{s_i} p_i)^2} - K e^{g(\mathbf{p})} \frac{\partial g(\mathbf{p})}{\partial p_i}, \quad (48)$$

where

$$\frac{\partial g(\mathbf{p})}{\partial p_i} = \frac{1}{K} \left( \frac{\sigma_s^2}{\sigma_s^2 p_i + \lambda_{s_i} p_i^2} - \frac{1}{M_s} \frac{\lambda_{c_i}}{\sigma_c^2 + \lambda_{c_i} p_i} \right).$$

Thus, the gradient of the objective  $\nabla h(\mathbf{p})$  can be obtained by

$$\nabla h(\mathbf{p}) = \begin{cases} \frac{\partial g(\mathbf{p})}{\partial p_i}, & i = 1, 2, \dots, K, \\ 0, & i = K + 1, \dots, N. \end{cases} \quad (49)$$

Denote  $\mathbf{p}^{(l)}$  as the feasible solution at the  $l$ -th iteration. While going a step forward along with the gradient direction, i.e.,  $\bar{\mathbf{p}}^{(l)} = \mathbf{p}^{(l)} + \alpha_1 \nabla h(\mathbf{p}^{(l)})$  may improve the objective value,  $\bar{\mathbf{p}}^{(l)}$  may not fall in the feasible set. The projection step onto the feasible set is essentially solving the following convex optimization problem

$$\tilde{\mathbf{p}}^{(l)} = \text{Proj}(\bar{\mathbf{p}}^{(l)}) = \arg \min_{\mathbf{x} \in \mathcal{F}} \|\mathbf{x} - \bar{\mathbf{p}}^{(l)}\|. \quad (50)$$

Thus, the feasible solution at the  $(l+1)$ -th iteration can be obtained by

$$\mathbf{p}^{(l+1)} = \mathbf{p}^{(l)} + \alpha_2^{(l)} (\tilde{\mathbf{p}}^{(l)} - \mathbf{p}^{(l)}). \quad (51)$$

where  $\alpha_2^{(l)}$  is the step size. By doing so, the optimal solution may be obtained after several iterations. The detailed algorithm procedure is summarized in Algorithm 3.

To visualize the effectiveness of the two proposed DW design algorithms, we take a low-dimensional case  $N = M_s = M_c = 2$  as an example. In such case, we can leverage exhaustive searching method to find the global optimal solution. To be specific, we collect the objective values over the 2-D grids  $p_1 \times p_2$ , where  $p_1, p_2 \in [0, P_T]$ . Fig. 3 shows that the optimal solution is achieved at the power bound, and the proposed two algorithms, namely, MI maximization and gradient projection both attain the optimal solution.

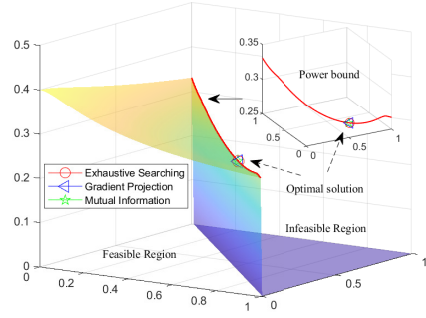


Fig. 3. The visualization of the DW waveform design for the case of  $N = M_s = M_c = 2$ ,  $\text{SNR}_s = 15$  dB,  $\text{SNR}_c = 0$  dB.

## VI. DISCUSSION

In this section, we will provide insights into the CAS waveform design by “tracking” the parameter’s uncertainties (i.e., variances) during the whole procedure. The original or prior variances of the equivalent independent parameters are denoted by  $\boldsymbol{\lambda} = [\lambda_1, \lambda_2, \dots, \lambda_N]$ , which are the eigenvalues of the covariance matrix  $\boldsymbol{\Sigma}_s$ .

*The SW scheme:* As shown in Fig. 4, in the sensing process, waver-filling algorithm is implemented to achieve the optimal MMSE. Here, the parameter variances are divided into two categories: 1) Small variances which remain constant (no power allocation) throughout the CAS procedure, and 2) relatively large variances where the MMSE is attained through power allocation, resulting in a variance of  $\sigma_s^2/\zeta_s$ . The water-filling factor  $\zeta_s$  is determined by the total power  $P_s$  allocated for the S-side. Consequently, we say that sensing process may reduce the uncertainties of the parameters.

In the communication process, the variances of the sources (estimates) are calculated by subtracting the MMSE from the original variances. The reverse water-filling algorithm is employed to minimize the distortion of the sources, with the reverse water-filling factor being chosen according to the achievable rate  $I_c$ . Indeed, the communication process may increase the uncertainties of the parameter acquired by sensing. In other words, the optimal MMSE estimation is attainable if the estimates can be transmitted losslessly, which implies a infinite channel capacity. We may observe that the final reduction of parameter uncertainties through the CAS equals to the reduction of the source variances during the communication process, i.e.,  $s_i - \xi$ .

*The DW scheme:* As depicted in Fig. 5, the DW design introduces a novel yet more intricate reverse water-filling problem. In the conventional scheme, the purpose of reverse water-filling is to minimize distortion with fixed variances and available information rates. However, in the DW scheme, the S-side and C-side are coupled w.r.t. the same waveform  $\mathbf{X}$ . This leads to the variances of the sources (estimates)  $\lambda_i(\mathbf{R}_n)$  related to  $\mathbf{X}$  and the MI  $I_c(\mathbf{X})$  (or the equivalent reverse water-filling factor  $\xi(\mathbf{X})$ ), evolve simultaneously. This inherent interdependency is the essential challenge in finding an optimal solution for the DW scheme.

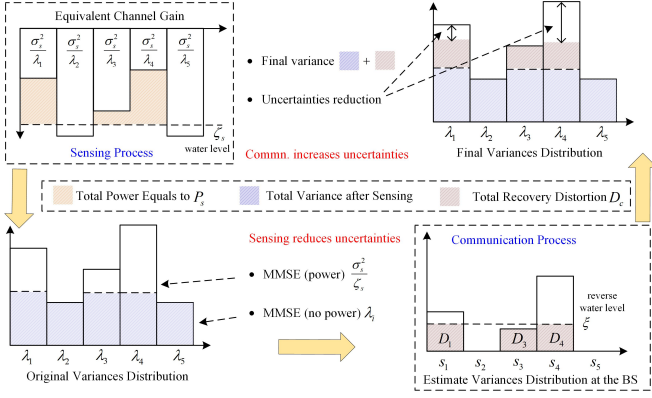


Fig. 4. The change of the parameter uncertainties in the SW strategy.

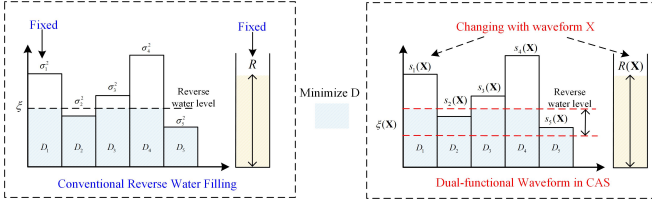


Fig. 5. The novel reverse water-filling problem introduced by the DW design.

**Remark 3:** In this paper, we exclusively focus on the comprehensible power allocation problem in the context of CAS systems. It is crucial to emphasize that system resources including bandwidth and dwell time, in addition to power, may also influence the performance of the SW and DW strategies, leading to distinct performance tradeoffs. Furthermore, the waveform designs for the radar parameter estimation with specific distributions and the networked sensing with task-based quantization, as well as the pursuit of more efficient algorithms for the DW design are also interesting topics, that are left for our future research.

## VII. SIMULATION RESULTS

In this section, we evaluate the effectiveness of the proposed waveform design strategies through numerical simulations. Unless otherwise specified, the system parameters are set as follows. The BS is equipped with  $N = 10$  transmitting antennas, while the number of receiving antennas at the S-side and C-side are set as  $M_s = M_c = 5$ . The total number of transmit symbols is  $T = 100$ . The communication channel is modeled by Rayleigh fading, where each entry of  $\mathbf{H}_c$  obeys the standard complex Gaussian distribution. Additionally, the sensing channel variance matrix is generated by [29]

$$\mathbb{E}[\mathbf{h}\mathbf{h}^H] = \mathbf{I}_{M_s} \otimes \Sigma_s = \mathbf{I}_{M_s} \otimes \sum_k \delta_k^2 \mathbf{a}(\theta_k) \mathbf{a}^H(\theta_k), \quad (52)$$

where  $\mathbf{a}(\theta_k) = \frac{1}{\sqrt{N}}[1, e^{j\pi \sin(\theta_k)}, \dots, e^{j\pi N \sin(\theta_k)}]$  and  $\delta_k$  represent the transmitting array steering vector and the expectation of the path-loss for the  $k$ -th path, respectively. Without loss of generality, we set  $\delta_k = 1$  and randomly choose  $K = 10$  angles over the interval  $[-90^\circ, 90^\circ]$ . Moreover, we use the normalized transmit power  $P_T = T$  and define the signal to noise ratio (SNR) by  $\text{SNR} = 10 \log(P_T/\sigma^2)$  dB.

### A. Evaluation of the SW Design

In the scenario of the SW design, the power distribution among the subchannels and objective value are determined with a given power allocated for the S-side  $P_s$ , or equivalent that for the C-side  $P_T - P_s$ . Therefore, we illustrate the tradeoff in performance between S&C by presenting the curves of sensing QoS versus power allocated for the S-side, where the sensing QoS is defined as the average distortion  $D/N$ .

Let us begin by examining the specific case of i.i.d. sensing subchannels with  $\lambda_s = 1$ . The SNR for the sensing channel is set at a constant value of  $\text{SNR}_s = 20$  dB. Meanwhile, we vary SNR for the communication channel  $\text{SNR}_c$  from 0 dB to 20 dB in increments of 5 dB. At first glance, Fig. 6(a) confirms the statement in Proposition 2 that the objective function is convex w.r.t.  $P_s$ . Therefore, the proposed one-dimensional search algorithm can effectively find the optimal solution. On one hand, we observe a discernible *power allocation tradeoff*. This tradeoff manifests when allocating excessive power to either side, resulting in significant performance degradation, until the achieved distortion is equal to the sum of prior variances. On the other hand, more power tends to be allocated to the S-side as the communication SNR level increases. This observation suggests that the BS tends to acquire more accurate parameter estimates when the communication quality is sufficiently high.

In Fig. 6(b), we present the performance tradeoff analysis for the general case, where the sensing variance matrix is generated by random angles. To eliminate redundancy, within this simulation, we maintain a fixed communication SNR at 20 dB, while varying the sensing SNR from 0 dB to 20 dB. Similar to the observations in Fig. 6(a), it is evident that sensing QoS improves as the sensing SNR increases. It is noteworthy that when the sensing SNR reaches a sufficiently high level, the BS expends a greater portion of its resources to enhance the communication capabilities. Fig. 6(c) provides the detailed power distribution among the S&C subchannels, where the channel qualities are arranged in descending order. We can observe that, in situations characterized by low SNR, a higher proportion of power is allocated to the subchannels with superior quality, while power allocation tends to become more uniform as the SNR reaches sufficiently high levels.

### B. Evaluation of the DW Design

In this subsection, we evaluate the performance of two proposed algorithms designed for the DW strategies within the context of independent sensing subchannels. We retain only the eigenvalues of  $\mathbf{R}_s$  as the variances of the non-uniform independent sensing channel. Note that the modified gradient projection (MGP) algorithm is specifically tailored for this scenario. For the purpose of comparison, we present the performance of heuristic MI maximization (HMI) algorithm with two sets of weighting factors: one with  $L = 3$  grids encompassing three special solutions, i.e., the communication-optimal ( $\alpha = 0$ ), the sensing-optimal ( $\alpha = 1$ ), and the sum of S&C MI ( $\alpha = 0.5$ ); the other with  $L = 11$  grids to explore a wider range of weight combinations.

Fig. 7(a) illustrates the relationships between the sensing QoS and the S&C SNRs for various algorithms. We can

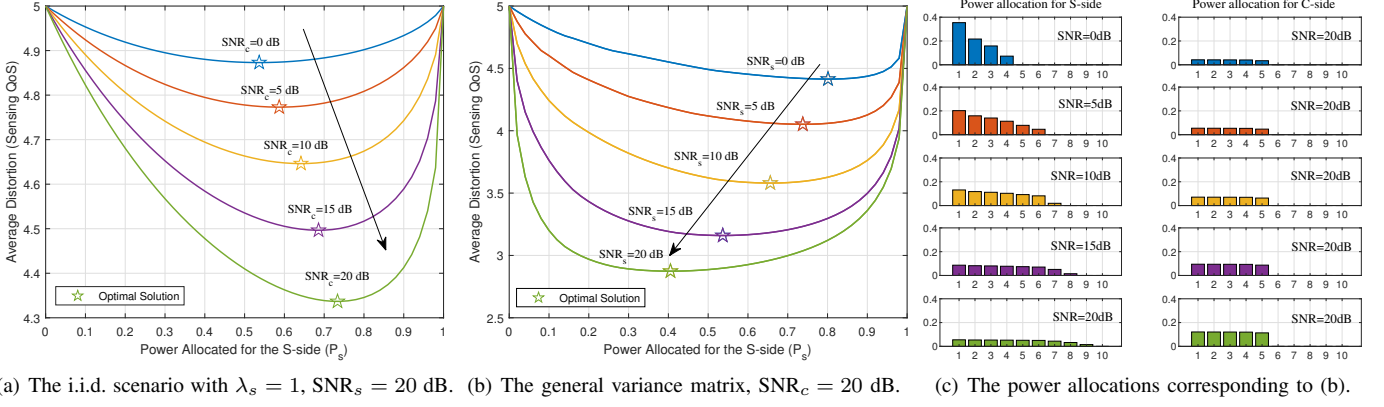


Fig. 6. The illustration of the SW design strategy: (a) Sensing QoS versus the power  $P_s$  for the i.i.d. sensing subchannels; (b) Sensing QoS versus the power  $P_s$  for the general sensing variance matrix; (c) Detailed power distributions among the subchannels.

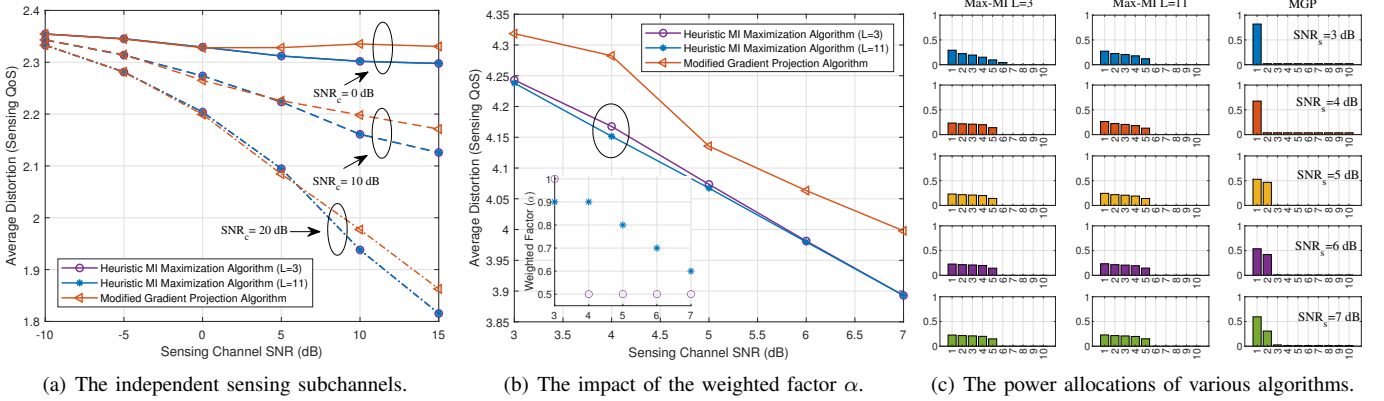


Fig. 7. The illustration of the DW design strategy: (a) Sensing QoS versus various S&C channel SNRs; (b) Impact of the weighted factor  $\alpha$  in MI maximization algorithm; (c) Detailed power distributions among the subchannels obtained by various algorithms.

observe three key phenomena as follows. 1) There is noticeable trend of improved sensing QoS with increasing S&C channel SNRs. 2) The HMI algorithm outperforms the MGP algorithm, due to the sensitivity of the MGP algorithm to the convexity of the objective function and the choice of the initial point. However, as observed in the 2D example, the objective function is not necessarily convex, resulting in a performance loss. 3) Interestingly, the HMI algorithm exhibits the same performance for both two sets of weight factors. This consistency can be attributed to the optimal weight factor, as detailed in Table I.

TABLE I  
THE OPTIMAL WEIGHTING FACTOR  $\alpha$ .

$\text{SNR}_c \backslash \text{SNR}_s$	-10 dB	-5 dB	0 dB	5 dB	10 dB	15 dB
0 dB	1	1	0	0	0	0
10 dB	1	1	1	0	0	0
20 dB	1	1	1	1	0	0

Surprisingly, the optimal weight factors for both sets consistently result in values of either 0 or 1 in this experiment. It implies that the optimal solution is achieved at either the sensing-optimal or the communication-optimal point. This

phenomenon can be attributed to the rearrangement of the eigenvalues of both the S&C subchannels, e.g., in descending order, to align the qualities of the S&C subchannels consistently. This operation can be accomplished by adjusting the eigenvectors thanks to the absence of the *subspace trade-off* in this case. Accordingly, optimizing communication performance simultaneously improves the sensing performance, and vice versa. Furthermore, it is observed that either S-side and C-side with relatively poorer channel quality takes precedence for optimization, ensuring compliance with the SCT constraint.

TABLE II  
THE OPTIMAL WEIGHTING FACTOR  $\alpha$ ,  $\text{SNR}_c = 10$  dB.

$\text{SNR}_s$	3 dB	4 dB	5 dB	6 dB	7 dB
$L = 3$	1	0.5	0.5	0.5	0.5
$L = 11$	0.9	0.9	0.8	0.7	0.6

In Fig.7(b), the sensing SNR range is constrained within 3 dB to 7 dB, while the communication SNR remains fixed at 10 dB. It becomes evident that refining the grid resolutions of the weighting factor  $\alpha$  leads to an improvement of sensing QoS. It can be observed from Table II that the weighting factor  $\alpha$  may be achieved different values over the interval  $[0, 1]$

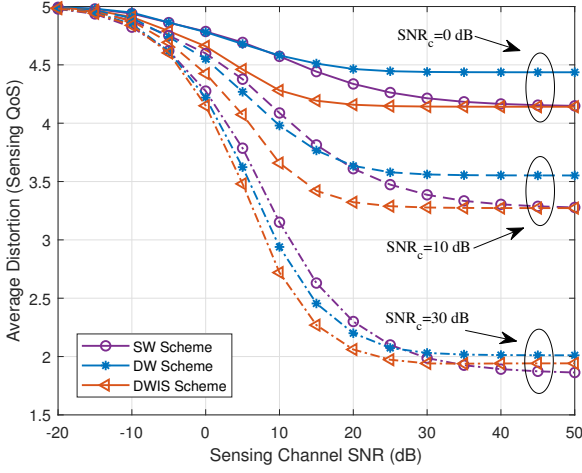


Fig. 8. The comparison of the SW and DW schemes.

when the qualities of the S&C subchannels are comparable. This clarifies the performance tradeoff between S-side and C-side. Moreover, the detailed power allocations for various algorithms are provided in Fig. 7(c), which elucidates distinct power allocation strategies.

### C. Comparison of the SW and DW Designs

Finally, we conduct a comparative analysis of the performance between the SW and DW designs within the context of CAS systems, while keeping the system conditions unchanged. To encompass a wide range of sensing channel qualities, we vary the sensing SNR from -20 dB to 50 dB. In addition to the SW and DW, we provide a benchmark scheme of the DW with independent sensing subchannel (DWIS), where the variances of the sensing subchannel are equal to the eigenvalues of  $\mathbf{R}_s$ . By providing the simulations of DWIS, we aim to demonstrate the impact of the *subspace tradeoff*.

As depicted in Fig. 8, it is evident that the DWIS scheme outperforms its counterparts. This superiority is attributed to the fact that the eigenspace of the waveform aligns perfectly with the optimal S&C subspaces, while simultaneously attaining a power multiplexing gain. Interestingly, the intersection points are observed between the SW and DW schemes in the moderate SNRs. In the regime of low SNRs, the power allocation between the S-side and C-side dominates the sensing QoS. Therefore, the DW outperforms the SW, benefiting from the resource multiplexing gains. Conversely, the performance of the SW surpasses the DW strategies when the S&C channels exhibit sufficiently high quality. As resource multiplexing gains approach saturation levels, the optimal waveform structures take precedence in influencing the sensing QoS. In the SW scheme, both S&C sides can be optimized simultaneously. This stands in contrast to the DW scheme due to the existence of *water-filling tradeoff*. Furthermore, the reordering of S&C subchannels qualities into a consistent order becomes unfeasible due to the presence of the *subspace tradeoff*, which results in a further performance loss.

## VIII. CONCLUSION

In this article, we developed a communication-assisted sensing (CAS) framework in 6G perceptive networks. Our framework is grounded in the principles of the rate-distortion theory and the source-channel separation theory in lossy data transmission. We conceived efficient waveform design algorithms tailored for two typical signaling strategies, namely, the separated sensing and communication (S&C) waveform and dual-function waveform, within the context of target response matrix estimation. Furthermore, we have conducted in-depth discussions of tradeoffs in power allocation for the separated S&C waveform, and the tradeoffs in subspace and water-filling for the dual-functional waveform. Our numerical simulations confirmed the effectiveness of the proposed algorithms. Meanwhile, the results highlight that the dual-function scheme outperforms the separated S&C scheme in the scenarios characterized by relatively poor channel conditions, as it capitalizes on the resource multiplexing gains. Conversely, the separated S&C scheme emerges as the preferable choice when the channel qualities reach a sufficiently high level.

### APPENDIX A

#### PROOF OF PROPOSITION 1

1) *Tightness of the SCT Constraint*: Assume that  $(\mathbf{p}_s^*, \mathbf{p}_c^*)$  is the optimal solution such that  $R(D_c) < I_c$ . The variance of source distribution  $\lambda_i(\mathbf{R}_\eta)$  is determined by  $\mathbf{p}_s^*$ . By recalling the non-increasing property of  $R(D)$  function, we can always improve the rate  $R$ , or equivalently reduce the distortion  $D_c$  in (28) through appropriately choosing the reverse water-filling factor  $\xi$  until reaching the communication achievable rate, namely,  $R(D_c) = I_c$ . Apparently, we have  $D_c(R) \geq D_c(I_c)$  if  $R \leq I_c$ . Note that this operation is irrelevant to the variables  $\tilde{\mathbf{p}}_s$  and  $\tilde{\mathbf{p}}_c$  but may further reduce the objective.

2) *Tightness of the Power Constraint*: Assume that  $(\mathbf{p}_s^*, \mathbf{p}_c^*)$  is the optimal solution such that  $\mathbf{1}_N^T(\mathbf{p}_s^* + \mathbf{p}_c^*) < P_T$ . Let us denote  $\Delta P$  as the residual power such that  $\mathbf{1}_N^T(\mathbf{p}_s^* + \mathbf{p}_c^*) + \Delta P = P_T$ . Then, we can always allocate the residual power to the C-side and obtain the new water-filling solution  $\tilde{\mathbf{p}}_c^*$  satisfying

$$\mathbf{1}_N^T \tilde{\mathbf{p}}_c^* = \mathbf{1}_N^T \mathbf{p}_c^* + \Delta P. \quad (53)$$

Then we have  $I_c(\tilde{\mathbf{p}}_c^*) \geq I_c(\mathbf{p}_c^*)$  due to the fact that the achievable rate is a monotonically non-decreasing function w.r.t. the power. Similarly, a smaller  $D_c$  can be attained by adjusting the reverse water-filling factor  $\xi$  such as  $R(D_c) = I_c(\tilde{\mathbf{p}}_c^*)$ . Consequently, the values of objective satisfies

$$D_s(\mathbf{p}_s^*) + D_c(\mathbf{p}_c^*) \geq D_s(\mathbf{p}_s^*) + D_c(\tilde{\mathbf{p}}_c^*), \quad (54)$$

which is contradicted to the assumption that  $(\mathbf{p}_s^*, \mathbf{p}_c^*)$  is the optimal solution. That completes the proof.

### APPENDIX B

#### PROOF OF PROPOSITION 2

Let us denote the objective function as

$$h(x) = (1 - e^{-g(x)})f(x) + \lambda_s e^{-g(x)}, \quad x \in [0, P_T]. \quad (55)$$



where  $g(x) = \frac{I_c(P_T - x)}{M_s N}$ . The first-order derivative of  $h(x)$  can be expressed by

$$h'(x) = f'(x) + [f(x)g'(x) - \lambda_s g'(x) - f'(x)]e^{-g(x)}. \quad (56)$$

Then, the second-order derivative is obtained by

$$h''(x) = (1 - e^{-g(x)})f''(x) + e^{-g(x)}(f(x) - \lambda_s)(g''(x) - (g'(x))^2). \quad (57)$$

In the first term, we have  $(1 - e^{-g(x)}) \geq 0$  due to  $g(x) \geq 0$  in the domain of  $x$ .  $f''(x) \geq 0$  since  $f(x)$  (i.e., the MMSE) is a convex function of  $x$ . In the second term, it is evident that  $f(x) - \lambda_s = -\lambda_\eta(x) \leq 0$  according to the definition (32c). We also have  $(g''(x) - (g'(x))^2) \leq 0$  since  $g''(x) \leq 0$  due to the fact that  $g(x)$  (i.e., the achievable rate) is the concave function of SNR [34]. Consequently, we have  $h''(x) \geq 0$  which indicates that  $h(x)$  is a convex function. That completes the proof.

## REFERENCES

- [1] F. Dong, F. Liu, S. Lu, W. Yuan, Y. Cui, Y. Xiong, and F. Gao, "Waveform design for communication-assisted sensing in 6g perceptive networks," in *2023 IEEE/CIC International Conference on Communications in China (ICCC)*, 2023, pp. 1–6.
- [2] A. Zhang, M. L. Rahman, X. Huang, Y. J. Guo, S. Chen, and R. W. Heath, "Perceptive mobile networks: Cellular networks with radio vision via joint communication and radar sensing," *IEEE Vehicular Technology Magazine*, vol. 16, no. 2, pp. 20–30, 2021.
- [3] Y. Cui, F. Liu, X. Jing, and J. Mu, "Integrating sensing and communications for ubiquitous iot: Applications, trends, and challenges," *IEEE Network*, vol. 35, no. 5, pp. 158–167, 2021.
- [4] ITU-R WP5D, "Draft New Recommendation ITU-R M. [IMT. FRAMEWORK FOR 2030 AND BEYOND]," 2023.
- [5] F. Liu, C. Masouros, A. P. Petropulu, H. Griffiths, and L. Hanzo, "Joint radar and communication design: Applications, state-of-the-art, and the road ahead," *IEEE Transactions on Communications*, vol. 68, no. 6, pp. 3834–3862, 2020.
- [6] J. A. Zhang, F. Liu, C. Masouros, R. W. Heath, Z. Feng, L. Zheng, and A. Petropulu, "An overview of signal processing techniques for joint communication and radar sensing," *IEEE Journal of Selected Topics in Signal Processing*, vol. 15, no. 6, pp. 1295–1315, 2021.
- [7] F. Liu, Y. Cui, C. Masouros, J. Xu, T. X. Han, Y. C. Eldar, and S. Buzzi, "Integrated sensing and communications: Toward dual-functional wireless networks for 6g and beyond," *IEEE Journal on Selected Areas in Communications*, vol. 40, no. 6, pp. 1728–1767, 2022.
- [8] K. Meng, Q. Wu, S. Ma, W. Chen, K. Wang, and J. Li, "Throughput maximization for uav-enabled integrated periodic sensing and communication," *IEEE Transactions on Wireless Communications*, vol. 22, no. 1, pp. 671–687, 2023.
- [9] Y. Xiong, F. Liu, Y. Cui, W. Yuan, T. X. Han, and G. Caire, "On the fundamental tradeoff of integrated sensing and communications under gaussian channels," *IEEE Transactions on Information Theory*, vol. 69, no. 9, pp. 5723–5751, 2023.
- [10] A. Liu, Z. Huang, M. Li, Y. Wan, W. Li, T. X. Han, C. Liu, R. Du, D. K. P. Tan, J. Lu, Y. Shen, F. Colone, and K. Chetty, "A survey on fundamental limits of integrated sensing and communication," *IEEE Communications Surveys & Tutorials*, vol. 24, no. 2, pp. 994–1034, 2022.
- [11] M. Ahmadipour, M. Kobayashi, M. Wigger, and G. Caire, "An information-theoretic approach to joint sensing and communication," *IEEE Transactions on Information Theory*, vol. 70, no. 2, pp. 1124–1146, 2024.
- [12] F. Liu, W. Yuan, C. Masouros, and J. Yuan, "Radar-assisted predictive beamforming for vehicular links: Communication served by sensing," *IEEE Transactions on Wireless Communications*, vol. 19, no. 11, pp. 7704–7719, 2020.
- [13] W. Yuan, F. Liu, C. Masouros, J. Yuan, D. W. K. Ng, and N. González-Prelcic, "Bayesian predictive beamforming for vehicular networks: A low-overhead joint radar-communication approach," *IEEE Transactions on Wireless Communications*, vol. 20, no. 3, pp. 1442–1456, 2021.
- [14] Z. Du, F. Liu, W. Yuan, C. Masouros, Z. Zhang, S. Xia, and G. Caire, "Integrated sensing and communications for v2i networks: Dynamic predictive beamforming for extended vehicle targets," *IEEE Transactions on Wireless Communications*, vol. 22, no. 6, pp. 3612–3627, 2023.
- [15] X. Meng, F. Liu, C. Masouros, W. Yuan, Q. Zhang, and Z. Feng, "Vehicular connectivity on complex trajectories: Roadway-geometry aware isac beam-tracking," *IEEE Transactions on Wireless Communications*, pp. 1–1, 2023.
- [16] K. Meng, Q. Wu, W. Chen, and D. Li, "Sensing-assisted communication in vehicular networks with intelligent surface," *IEEE Transactions on Vehicular Technology*, vol. 73, no. 1, pp. 876–893, 2024.
- [17] F. Dong, F. Liu, Y. Cui, W. Wang, K. Han, and Z. Wang, "Sensing as a service in 6g perceptive networks: A unified framework for isac resource allocation," *IEEE Transactions on Wireless Communications*, vol. 22, no. 5, pp. 3522–3536, 2023.
- [18] F. Dong, F. Liu, Y. Cui, S. Lu, and Y. Li, "Sensing as a service in 6g perceptive mobile networks: Architecture, advances, and the road ahead," *IEEE Network*, pp. 1–1, 2024.
- [19] Q. Zhang, X. Wang, Z. Li, and Z. Wei, "Design and performance evaluation of joint sensing and communication integrated system for 5g mmwave enabled cavs," *IEEE Journal of Selected Topics in Signal Processing*, vol. 15, no. 6, pp. 1500–1514, 2021.
- [20] M. Thomas and A. T. Joy, *Elements of information theory*. Wiley-Interscience, 2006.
- [21] T. Berger, Z. Zhang, and H. Viswanathan, "The CEO problem [multiterminal source coding]," *IEEE Transactions on Information Theory*, vol. 42, no. 3, pp. 887–902, 1996.
- [22] Y. Oohama, "Indirect and direct Gaussian distributed source coding problems," *IEEE Transactions on Information Theory*, vol. 60, no. 12, pp. 7506–7539, 2014.
- [23] A. Kipnis, S. Rini, and A. J. Goldsmith, "The rate-distortion risk in estimation from compressed data," *IEEE Transactions on Information Theory*, vol. 67, no. 5, pp. 2910–2924, 2021.
- [24] Y. Oohama, "The rate-distortion function for the quadratic Gaussian CEO problem," *IEEE Transactions on Information Theory*, vol. 44, no. 3, pp. 1057–1070, 1998.
- [25] V. Prabhakaran, D. Tse, and K. Ramachandran, "Rate region of the quadratic Gaussian CEO problem," in *International Symposium on Information Theory, 2004. ISIT 2004. Proceedings.*, 2004, p. 119.
- [26] E. Ekrem and S. Ulukus, "An outer bound for the vector gaussian ceo problem," in *2012 IEEE International Symposium on Information Theory Proceedings*, 2012, pp. 576–580.
- [27] S. Rini, A. Kipnis, R. Song, and A. J. Goldsmith, "The compress-and-estimate coding scheme for Gaussian sources," *IEEE Transactions on Wireless Communications*, vol. 18, no. 9, pp. 4344–4356, 2019.
- [28] K. Eswaran and M. Gastpar, "Remote source coding under gaussian noise: Dueling roles of power and entropy power," *IEEE Transactions on Information Theory*, vol. 65, no. 7, pp. 4486–4498, 2019.
- [29] B. Tang and J. Li, "Spectrally constrained MIMO radar waveform design based on mutual information," *IEEE Transactions on Signal Processing*, vol. 67, no. 3, pp. 821–834, 2019.
- [30] Y. Yang and R. S. Blum, "MIMO radar waveform design based on mutual information and minimum mean-square error estimation," *IEEE Transactions on Aerospace and Electronic Systems*, vol. 43, no. 1, pp. 330–343, 2007.
- [31] S. M. Kay, *Fundamentals of statistical signal processing: Estimation theory*. Englewood Cliffs, NJ: Prentice-Hall, 1993.
- [32] S. Lu, F. Liu, F. Dong, Y. Xiong, J. Xu, Y.-F. Liu, and S. Jin, "Random isac signals deserve dedicated precoding," *arXiv preprint arXiv:2311.01822*, 2023.
- [33] F. Dong, F. Liu, S. Lu, and Y. Xiong, "Rethinking estimation rate for wireless sensing: A rate-distortion perspective," *IEEE Transactions on Vehicular Technology*, pp. 1–6, 2023.
- [34] D. Guo, S. Shamai, and S. Verdú, "Mutual information and minimum mean-square error in gaussian channels," *IEEE Transactions on Information Theory*, vol. 51, no. 4, pp. 1261–1282, 2005.